


# Combination of Indomethacin with Nanostructured Lipid Carriers for Effective Anticancer Therapy

Vaikunthivasan Thiruchenthooran <sup>1</sup>, Marta Espina <sup>2,3</sup>, Marta Świtalska<sup>4</sup>, Lorena Bonilla-Vidal<sup>2,3</sup>, Joanna Wietrzyk <sup>4</sup>, Maria Luisa Garcia <sup>2,3</sup>, Eliana B Souto<sup>5</sup>, Elena Sánchez-López <sup>2,3,6,\*</sup>, Anna Gliszczynska <sup>1,\*</sup>

<sup>1</sup>Department of Food Chemistry and Biocatalysis, Wrocław University of Environmental and Life Sciences, Wrocław, Poland; <sup>2</sup>Department of Pharmacy, Pharmaceutical Technology and Physical Chemistry, University of Barcelona, Barcelona, Spain; <sup>3</sup>Institute of Nanoscience and Nanotechnology (IN<sup>2</sup>UB), University of Barcelona, Barcelona, Spain; <sup>4</sup>Department of Experimental Oncology, Ludwik Hirszfeld Institute of Immunology and Experimental Therapy, Polish Academy of Sciences, Wrocław, Poland; <sup>5</sup>Laboratory of Pharmaceutical Technology, Department of Drug Sciences, Faculty of Pharmacy, University of Porto, Porto, Portugal; <sup>6</sup>Unit of Synthesis and Biomedical Applications of Peptides, IQAC-CSIC, Barcelona, Spain

\*These authors contributed equally to this work

Correspondence: Anna Gliszczynska; Elena Sánchez-López, Email [anna.gliszczynska@upwr.edu.pl](mailto:anna.gliszczynska@upwr.edu.pl); [esanchezlopez@ub.edu](mailto:esanchezlopez@ub.edu)

**Purpose:** The anticancer potential of indomethacin and other nonsteroidal anti-inflammatory drugs (NSAIDs) in vitro, in vivo, and in clinical trials is well known and widely reported in the literature, along with their side effects, which are mainly observed in the gastrointestinal tract. Here, we present a strategy for the application of the old drug indomethacin as an anticancer agent by encapsulating it in nanostructured lipid carriers (NLC). We describe the production method of IND-NLC, their physicochemical parameters, and the results of their antiproliferative activity against selected cancer cell lines, which were found to be higher compared to the activity of free indomethacin.

**Methods:** IND-NLC were fabricated using the hot high-pressure homogenization method. The nanocarriers were physicochemically characterized, and their biopharmaceutical behaviour and therapeutic efficacy were evaluated in vitro.

**Results:** Lipid nanoparticles IND-NLC exhibited a particle size of 168.1 nm, a negative surface charge (−30.1 mV), low polydispersity index (PDI of 0.139), and high encapsulation efficiency (over 99%). IND-NLC were stable for over 60 days and retained integrity during storage at 4 °C and 25 °C. The potential therapeutic benefits of IND-NLC were screened using in vitro cancer models, where nanocarriers with encapsulated drug effectively inhibited the growth of breast cancer cell line MDA-MB-468 at dosage 15.7 μM.

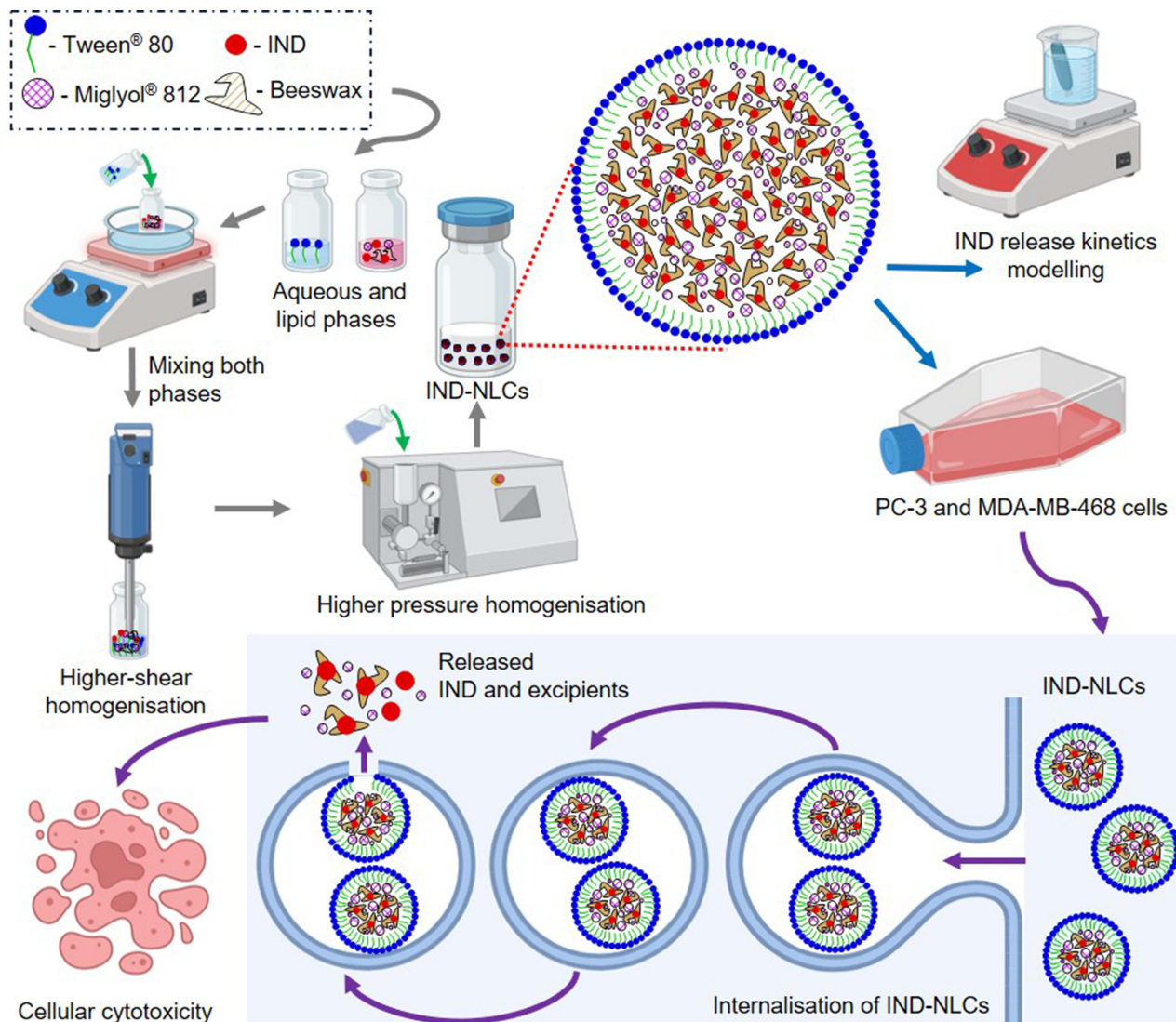
**Conclusion:** We successfully developed IND-NLC for delivery of indomethacin to cancer cells and confirmed their antitumoral efficacy in in vitro studies. The results suggest that indomethacin encapsulated in lipid nanoparticles possesses high anticancer potential. Moreover, the presented strategy is highly promising and may offer a new alternative for future therapeutic drug innovations.

**Keywords:** lipid nanoparticles, indomethacin, antitumoral activity, tumor-targeting

## Introduction

Cancer plays a leading role in the death rate worldwide and poses a major challenge to global healthcare due to its numerous subtypes and genetic variability. In 2022, nearly 9.7 million people died from cancer, while the projected scale of new cases is expected to increase and reach 35 million by 2050.<sup>1</sup> With enhancement in cancer-related morbidity and mortality, there is an increasing need to search for new effective drugs and therapies. However, the development of new anticancer drugs requires extensive research, procedures are expensive and carry the risk of low success rate. The average cost of new drug development is estimated around \$648 million (range between \$157.3 - \$1950.8 million) and the time required for approval and marketing takes 10 to 17 years.<sup>2</sup> Moreover, despite such a high expenditure of time and costs, less than 1% of studied compounds advanced towards clinical trials and market.<sup>2</sup> Both the European Medicines Agency (EMA)

## Graphical Abstract



and the American Food and Drug Administration (FDA) approve only a few de novo drugs every year. In 2021, 2022, and 2023, FDA released 50, 37, and 55 de novo drugs, respectively<sup>3</sup> while EMA approved only 54, 41, and 39 de novo drugs, respectively.<sup>4</sup> Taking these numbers into account, repurposing already accepted drugs with known safety profiles attracts the attention of researchers and industries worldwide. This method offers the advantages of rapid development of new therapies, lower treatment costs, and wider application of well-known drugs with defined side effects.<sup>5</sup>

Nonsteroidal anti-inflammatory drugs (NSAIDs) have been used for more than four decades as effective chemotherapeutic agents in the *in vitro*, *in vivo* and epidemiological studies.<sup>6</sup> The first mention about NSAIDs applications for cancer appeared in the 80s.<sup>7</sup> Inflammation is a natural part of the body's immune response, but chronic or prolonged inflammation is often responsible for development in the organism of various diseases, including cancer. Some studies suggest that the long-term administration of NSAIDs may protect against the development of certain types of cancers. For instance, it is reported that intake of NSAIDs like aspirin, indomethacin (IND), ibuprofen, mefenamic acid, or piroxicam four times per week for three months reduces stomach cancer (but causes other side-effects).<sup>8</sup> NSAIDs are

reported as potential chemotherapeutic agents able to induce apoptosis of cancer cells and inhibit their proliferation and angiogenesis, resulting in the reduction of tumor growth.<sup>9</sup>

Among several NSAIDs is a non-selective COX-2 inhibitor that exhibits analgesic and antipyretic properties. Its mechanism of action on the molecular level is still not fully understood. IND is widely used in the United States as an effective agent able to reduce pain, fever, and inflammation.<sup>10</sup> Moreover, antitumoral effects of IND have also been studied indicating the ability to reduce the size and number of tumors.<sup>8,11</sup> It is well known that IND possess low water solubility and its intake leads to several side effects on the gastrointestinal tract. Therefore, many attempts have been made to overcome these limitations. One of them is the application of nanotechnology for the development of new formulations.

Nanotechnology is shown to be essential in the advancement of innovative anti-cancer treatments. Nanoparticle-based drug delivery offers several advantages over conventional dosage forms, including improved pharmacokinetics, specific targeting of tumor cells, and reduced drug resistance and serious adverse effects.<sup>12,13</sup> Moreover, nanotechnology offers the possibility to deliver poorly soluble drugs into tumor tissues.<sup>14</sup> Up to date, a liposomal formulation of indomethacin (IND-Lip) was successfully developed by Gupta and co-workers<sup>15</sup> and demonstrated superior efficacy in comparison to the free drug. IND-Lip was obtained in the form of negatively charged monodispersed vesicles and was tested for lung adenocarcinomas, exhibiting almost two-fold higher activity than free IND towards the cancer cell line A549 with an IC<sub>50</sub> 38.4 μM.<sup>15</sup> Indomethacin-loaded solid lipid nanoparticles (IND-SLNs) developed for ocular delivery also demonstrated improved chemical stability and increased in vitro corneal permeability.<sup>16</sup> Moreover, Majumdar and co-workers<sup>17</sup> studied solid lipid nanoparticles (SLN) and nanostructured lipid carriers (NLC) loaded with IND for ocular delivery and evaluated the distribution of IND after topical administration of produced formulations. They confirmed that lipid-based nanoparticles are effective vehicles for ocular delivery, demonstrating increased drug-loading capability and suitable delivery to the anterior and posterior ocular segments.<sup>17</sup>

NLC are the second generation of lipid nanoparticles and constitute an effective alternative over liposomes and other colloidal carriers used in the pharmaceutical field. NLCs are composed of a blend of solid and liquid lipids, which leads to the formation of a specific nanostructure with increased drug loading capacity. These nanoparticles can be loaded with anticancer agents, enabling their use in the form of oral therapy. NLCs are produced from materials generally recognized as safe (GRAS), have the ability to load, in particular, lipophilic and poorly water-soluble drugs, and are easy to scale-up.<sup>18–20</sup>

The aim of this work was then to develop new nanostructured lipid carriers (NLC) for the effective delivery of indomethacin with increased anticancer activity. NLC loaded with indomethacin (IND-NLC) were fabricated and physicochemically characterized. In this work, we encapsulated IND using beeswax as the solid lipid to enhance IND cytotoxic activity due to its anticancer properties.<sup>21,22</sup> Next, the antiproliferative activity of IND-NLC against two types of selected cancer cells, namely, breast (MDA-MB-468) and prostate (PC-3) cell lines, was evaluated as well as cellular internalisation. The antitumoral efficacy of IND-NLC was demonstrated in vitro. IND-NLC was active against PC-3 and MDA-MB-468 cancer cells at 74.1 and 15.7 μM, respectively, whereas free IND did not show tumoral activity.

## Materials and Methods

Indomethacin (IND), Tween<sup>®</sup> 80 (polysorbate 80), Beeswax, Nile Red (NR), and orthophosphoric acid (85%) were obtained from Sigma-Aldrich (Madrid, Spain). Urea and sodium citrate tri-base were obtained from Montplet & Esteban SA (Madrid, Spain), Miglyol<sup>®</sup> 812 from Roig Farma SA (Madrid, Spain), and methanol (99.8%, HPLC grade) from Fisher Scientific (Geel, Belgium). Ethanol (99.8%, Analytical grade) was obtained from PanReac AppliChem (Barcelona, Spain). Deionized water was generated from the Millipore<sup>®</sup> Milli<sup>®</sup> Q system and was used in all formulations and experiments.

## Preparation of Nanostructured Lipid Carriers

The hot high-pressure homogenization (HPH) technique was selected for the production of blank (NLC) and loaded indomethacin nanostructured lipid carriers (IND-NLC), following a previously described procedure.<sup>23</sup> This method has

the advantage of easy scale-up at industrial level. Briefly, the lipid phase containing beeswax (solid lipid, melting point: 65.9 °C) and Miglyol® 812 (liquid lipid) was heated at 85 °C in a water bath. The lipid phase was prepared by melting a certain amount of beeswax mixed with Miglyol® 812, whereas the aqueous phase, composed of water and Tween® 80 (surfactant), was heated at the same temperature. IND-NLC were produced by following the same procedure as NLC, but IND was dissolved in the lipid phase prior to emulsification. The primary emulsion was formed by mixing the aqueous phase with the lipid phase at the same temperature, followed by high-shear homogenization using an Ultra-Turrax® T10 basic (IKA®, Staufen, Germany) for 30s, at the speed of 8000 rpm. The obtained emulsions were then subjected to high-pressure homogenisation at 85 °C for three homogenisation cycles at 900 bar. Both empty NLC and IND-NLC were stored at room temperature.

Fabrication of Nile Red (NR)-labelled NLC (IND-NLC-NR) was performed as described for the production of IND-NLC, but adding 0.04% (w/w) of NR to the inner lipid phase.<sup>24</sup>

## Characterization of Indomethacin-Loaded Nanocarriers

### Determination of Particle Size, Polydispersity Index, and Zeta Potential

The Dynamic Light Scattering (DLS) technique was used to assess the particle size (Z-Ave) and polydispersity index (PDI) of the fabricated IND-NLC. The measurements were taken after diluting the IND-NLC with Milli-Q water at a ratio of 1:10. The zeta potential (ZP) was determined by employing a Zetasizer Nano ZS (Malvern Instruments, Malvern, UK) following a dilution ratio of 1:20. The measurements were carried out in triplicate at a temperature of 25 °C and the results were reported as the mean ± standard deviation.<sup>25,26</sup>

### Encapsulation Efficiency

The encapsulation efficiency (EE) of IND was measured indirectly by quantifying the non-encapsulated IND in the IND-NLC. Free IND was separated from IND-NLC by ultrafiltration-centrifugation method at 14000 rpm for 15 minutes (Mikro 22 Microliter Centrifuge, Germany) using 100 kDa filters (Merck KGaA, Germany). Non-encapsulated IND was quantified by reverse-phase high-performance liquid chromatography (RP-HPLC) Waters 2695 system (Waters, Massachusetts, USA) using a Kromasil® Classic C18 column (5 µM × 4.6 mm × 150 mm) (Nouryon, Amsterdam, Netherlands). A photodiode array detector (Waters 2996, Waters, Milford, USA) at a wavelength of 220 nm was used to quantify IND. The mobile phase (1mL/min flow rate) consisted of a water phase containing orthophosphoric acid, and an organic phase consisting of methanol (20:80, v/v). Data was processed using the Empower® 3 software (Waters, USA).

EE was calculated as the ratio between the loaded IND (calculated by subtracting the free IND from the total amount of IND) and the total amount of IND weighted for the production (Equation 1). The analysis was performed in triplicate, and the results are presented as the mean ± standard deviation.

$$\%EE = \frac{\text{Total amount of IND} - \text{Free IND}}{\text{Total amount of IND}} \times 100 \quad (1)$$

### Transmission Electron Microscopy

The morphology of IND-NLC was analysed by transmission electron microscopy (TEM) in a Jeol 1010 microscope (JEOL, Massachusetts, USA). IND-NLC were firstly diluted in water (1:5) followed by negative staining using 2% of uranyl acetate. Imaging was performed on a copper grid surface activated by UV light.

### Interaction Studies

#### Differential Scanning Calorimetry

Thermograms of air-dried samples were recorded in a differential scanning calorimetry DSC 823e system (Mettler-Toledo 4000 system, Mettler-Toledo, Barcelona, Spain). The samples were placed in perforated aluminum pans and weighted using a Mettler M3 Microbalance (Mettler Toledo, Greifensee, Switzerland). Thermograms of IND, NLC, and IND-NLC were recorded under a nitrogen atmosphere by subjecting them to a heating ramp from 25 °C to 200 °C at



a rate of 10 °C per minute. The calorimetric system was calibrated using a pan containing indium (Fluka, Switzerland) with a purity of at least 99.95%. An empty aluminum pan was utilized as a point of reference. The collected data were analysed in a Mettler STARe V 9.01 dB (Mettler-Toledo, Barcelona, Spain).

## X-Ray Diffraction

X-ray diffraction (XRD) diffractograms of IND and air-dried NLC and IND-NLC formulations were evaluated by placing them between two polyester films having a thickness of 3.6 µm. They were then exposed to CuK α radiation with a voltage of 45 kV, a current of 40 mA, and a wavelength of 1.5418 Å. The measurements were conducted at 2θ values ranging from 2° to 60°, with a step size of 0.026°. Each step interval lasted for 200 seconds.

## Fourier Transform Infrared Spectroscopy

The Fourier transform infrared (FTIR) spectra of air-dried IND-NLC were analysed in a Thermo Scientific Nicolet iZ10 spectrometer equipped with a diamond ATR crystal and a DTGS detector (Thermo Scientific, Barcelona, Spain). Infrared spectra were analyzed in the 500–4000 cm<sup>-1</sup> regions with 1 cm<sup>-1</sup> resolution.

## Storage Stability

IND-NLC stability was analyzed at three temperatures: in a refrigerator (4 °C), at room temperature (25 °C), and at high temperatures (37 °C). This study was carried out by examining the light backscattering profiles of IND-NLC utilizing a Turbiscan<sup>®</sup> Lab (IESMAT, Spain). To achieve this objective, a glass measurement cell was filled with the sample and thereafter stored at various temperatures. The light source used was a pulsed near-infrared LED with a wavelength of 880 nm. It was detected by a backscattering detector placed at an angle of 45° relative to the incident beam. The BS profile of IND-NLC was analyzed at 0, 30, and 60 days for 24 h at 1 h intervals. At the same time points, the Z-Ave, PDI, and ZP of IND-NLC were also measured using a Zetasizer Nano ZS. These experiments were carried out in duplicate, and visual observations of the samples were performed.

## Sterilization by Gamma Radiation

IND-NLC was sterilized using gamma irradiation at a dose of 25 kGy <sup>60</sup>Co (Aragogamma, Barcelona, Spain). The effect of gamma irradiation was studied by analysing physicochemical parameters (Z-Ave, PDI, and ZP) and evaluating EE before and after gamma radiation.

## In vitro Drug Release

The release of IND from IND-NLC was evaluated in vitro using dialysis cassettes with a molecular weight cut-off of 10 K (MWCO, Slide-A-Lyzer<sup>™</sup>, Thermo Scientific, Rockford, USA).<sup>27</sup> The release of IND was quantified by comparing it to the concentration of IND using a 500 µL dialysis cassette. The acceptor compartment consisted of water-jacketed glass cells and was incubated at 37 °C. The release medium was equilibrated at pH 7 and included sodium citrate (0.45%, w/v) and urea (1.05%, w/v) to ensure the sink conditions.<sup>28</sup> At specific time intervals, 400 µL aliquots were withdrawn and immediately replaced by fresh release medium. The collected samples were analysed using RP-HPLC. The release kinetics of IND were plotted as the cumulative IND release (%) vs time (h) using Graph Pad Prism 8.0 software and fitted to the most common kinetic models using Equations 2–6.<sup>29</sup>

Zero-order equation:

$$\frac{Q_t}{Q_\infty} (\%) = K_0 t \quad (2)$$

First-order equation:

$$\frac{Q_t}{Q_\infty} (\%) = 1 - e^{-K_1 t} \quad (3)$$

Hyperbola equation:

$$\frac{dQ}{dt} = \frac{V_m Q}{(K_m + Q)} \quad (4)$$

Higuchi equation:

$$\frac{Q_t}{Q_\infty} (\%) = K_h t^{1/2} \quad (5)$$

Korsmeyer-Peppas equation:

$$\frac{Q_t}{Q_\infty} (\%) = K_{kp} t^n \quad (6)$$

Where  $Q_t/Q_\infty$  represents the percentage fraction of drug content released at time (t);  $K_0$  and  $K_f$  represent the zero- and first-order release rate constants, respectively;  $V_m$  represents the maximum speed of release;  $K_m$  represents the drug content at which the release velocity is half maximum;  $K_h$  and  $K_{kp}$  represent the constants of Higuchi and Korsmeyer-Peppas release rate, respectively; and  $n$  represents the drug release exponent.

## Cell Lines

The PC-3 cell line, derived from human prostate cancer, was obtained from the European Collection of Authenticated Cell Cultures (UK). The MDA-MD-468 cell line, a human breast cancer cell, was obtained from the Leibniz Institute DSMZ German Collection of Microorganisms and Cell Culture (Germany). The cell lines were cultured and preserved at the Hirszfeld Institute of Immunology and Experimental Therapy (Polish Academy of Science, Wroclaw, Poland). The cell lines were grown in a combination of RPMI 1640 +GlutaMAX media (Gibco, UK) supplemented with 10% fetal bovine serum (FBS) for PC-3 cells and 20% FBS for MDA-MB-468 cells (HyClone, Cytiva). The culture media were supplemented with 100 µg/mL of streptomycin (Merck, Germany) and 100 units/mL of penicillin (Polfa Tarchomin S.A., Poland).

## Determination of Antiproliferative Activity of Fabricated Nanoformulations Towards Selected Human Cancer Cell Lines

Antiproliferative activity of IND, NLC, and IND-NLC were examined using SRB assay after 24 and 48 hours of exposure.<sup>30</sup> IND and IND-NLC were diluted based on the %EE of IND (1.51 mg/mL) and were assayed between 0.8 and 100 µM. The same dilutions were applied for empty NLC. Before testing the samples (IND, NLC, and IND-NLC), the cells were placed in 96-well plates (Sarstedt, Germany) at a density of  $1 \times 10^4$  cells per well and cultured for 24 hours. The results were computed individually as the IC<sub>50</sub>, which is the concentration at which 50% of the cells are cytotoxic. The IC<sub>50</sub> values were individually determined for each experiment using the Prolab-3 system, utilizing the Cheburator 0.4 software. The mean values, together with their corresponding standard deviation (SD), were then reported.<sup>31</sup> Each concentration of every sample was subjected to three replicates in a single experiment, which was repeated between three and five times.

## Determination of Nanocarriers Accumulation in Cells by Flow Cytometry

IND-NLC were fluorescently labelled with NR (IND-NLC-NR) to determine their accumulation in cells. Prostate PC-3 and breast cancer MDA-MB-468 cells were incubated with IND-NLC-NR (20 µM) for 5, 15, 30, 60, 120, and 240 minutes. Following the incubation period, the cells were collected and rinsed with PBS. The average fluorescence of cells treated with the particles labeled with NR was assessed using flow cytometry in a BD LSRFortessa cytometer (BD Bioscience, San Jose, USA). Unlabeled controls were created using untreated cells. The results were evaluated in the Flowing software 2 (Cell Imaging Core, Turku Centre for Biotechnology, University of Turku Åbo Akademi University).

## Statistics

Student's *t*-tests were performed for a two-group comparison to indicate significance among the treatments using Statgraphics 18. Differences were considered statistically significant at  $p \leq 0.05$ . The statistical analysis for two-group comparisons, NLC vs IND-NLC, was performed by using non-parametric Mann–Whitney test, GraphPad Prism 7. Statistically significant differences were considered at  $p \leq 0.05$ .

## Results

### Characterization of Nanocarriers with Encapsulated Indomethacin

Beeswax was selected according to previously reported data as a solid lipid for solubilisation of IND.<sup>23</sup> Average particle size (*Z*-Ave) of empty NLC and IND-NLC was determined as  $155.3 \pm 3.2$  nm and  $168.1 \pm 0.6$  nm, respectively. Both formulations contained monomodal populations with polydispersity index (PDI) below 0.2. The polydispersity value of NLC was 0.162, whereas of IND-NLC was 0.139. Both empty NLC and IND-NLC were anionic with negative ZP values of  $-21.1 \pm 0.6$  mV and  $-30.1 \pm 0.7$  mV, respectively. The EE of IND-NLC was high, being able to encapsulate almost all IND ( $99.44\% \pm 0.02$ ).

Morphological analysis of the optimised IND-NLC using TEM revealed that the nanoparticles were non-aggregated with a spherical shape, and sizes below 200 nm (Figure 1A).

DSC was performed to investigate the interactions between the drug and the lipid matrix (Figure 1B). The thermograms revealed that IND exhibited a distinct endothermic melting peak at 164 °C, while NLC and IND-NLC displayed endothermic peaks at 64 °C and 59 °C, respectively. The absence of the melting peak of IND in the DSC thermogram of the IND-NLC suggests that the drug was uniformly distributed at a molecular level within the NLC matrix, and dissolved within the lipid matrix. Additionally, a little change in the temperature at which the NLC started to melt was detected in the IND-NLC, with the melting peak shifting from 64 °C to 59 °C.

XRD was performed to confirm the crystallinity of NLC and IND-NLC. The XRD diffractograms (Figure 1C) showed the physical state of IND in its crystalline form, expressed by sharp diffraction peaks at 10.2°, 11.8°, 17.0°, 19.9°, and 21.9° (2 $\theta$ ) corresponding to the  $\gamma$ -polymorph and the purity of IND.<sup>32</sup> NLC and IND-NLC diffractograms present two peaks at 21.4° and 23.8° (2 $\theta$ ), indicating the second stable form of triacylglycerols, the  $\beta'$  form.<sup>33</sup> The absence of IND peaks in IND-NLC confirms that the drug was dissolved in the NLC (molecular dispersion).

ATR-FTIR was used to evaluate the molecular interactions between drug, the lipid matrix, and surfactant (Figure 1D). The FTIR spectrum of pure IND presented characteristic bands at 1716 and 1690  $\text{cm}^{-1}$  assigned to the carbonyl group in the carboxyl group (C=O), and at 1479  $\text{cm}^{-1}$  from the aromatic ring (C=C). Additional bands between 1262 and 1221, below 1012, and at 737  $\text{cm}^{-1}$  were attributed to the ether group (=C-O), deformation bonds (C-H), and stretching bonds between carbon and halogen atoms (C-Cl), respectively.<sup>34</sup>

The ATR-FTIR spectra of IND-NLC indicated that they did not show the formation of new covalent bonds.

### Storage Stability

Storage stability study performed at 4, 25, and 38 °C was carried out with IND-NLC by monitoring the particle size (Figure 2A), PDI (Figure 2A), ZP (Figure 2B), and back scattering ( $\Delta$ BS) profiles (Figure 2C–E).

IND-NLC were stable at 4 °C and 25 °C for 2 months, and no significant differences ( $p > 0.05$ ) in particle size and PDI were observed (Figure 2A). Statistical differences ( $p \leq 0.05$ ) in these parameters were observed at higher temperatures when particle destabilisation occurred (Figure 3B). Particle size decreased from  $172.3 \text{ nm} \pm 1.65$  (1st day) to  $160 \pm 2.04$  nm (60th day), whereas ZP from  $-28.6$  mV to  $-16.1$  mV. These observations are in accordance with the BS results (Figure 2C–E) where at 38°C the BS profile (Figure 2E) increased, probably as a result of a degradation process.

### Sterilization

NLC and IND-NLC were sterilised using a <sup>60</sup>Co radiation source.<sup>35</sup> Physicochemical changes were analyzed to determine whether the sterilization process could influence the particle size and PDI (Figure 3A), as well as ZP and %EE (Figure 3B). The results indicated that radiation did not significantly affect these parameters. IND-NLC particle size slightly decreased

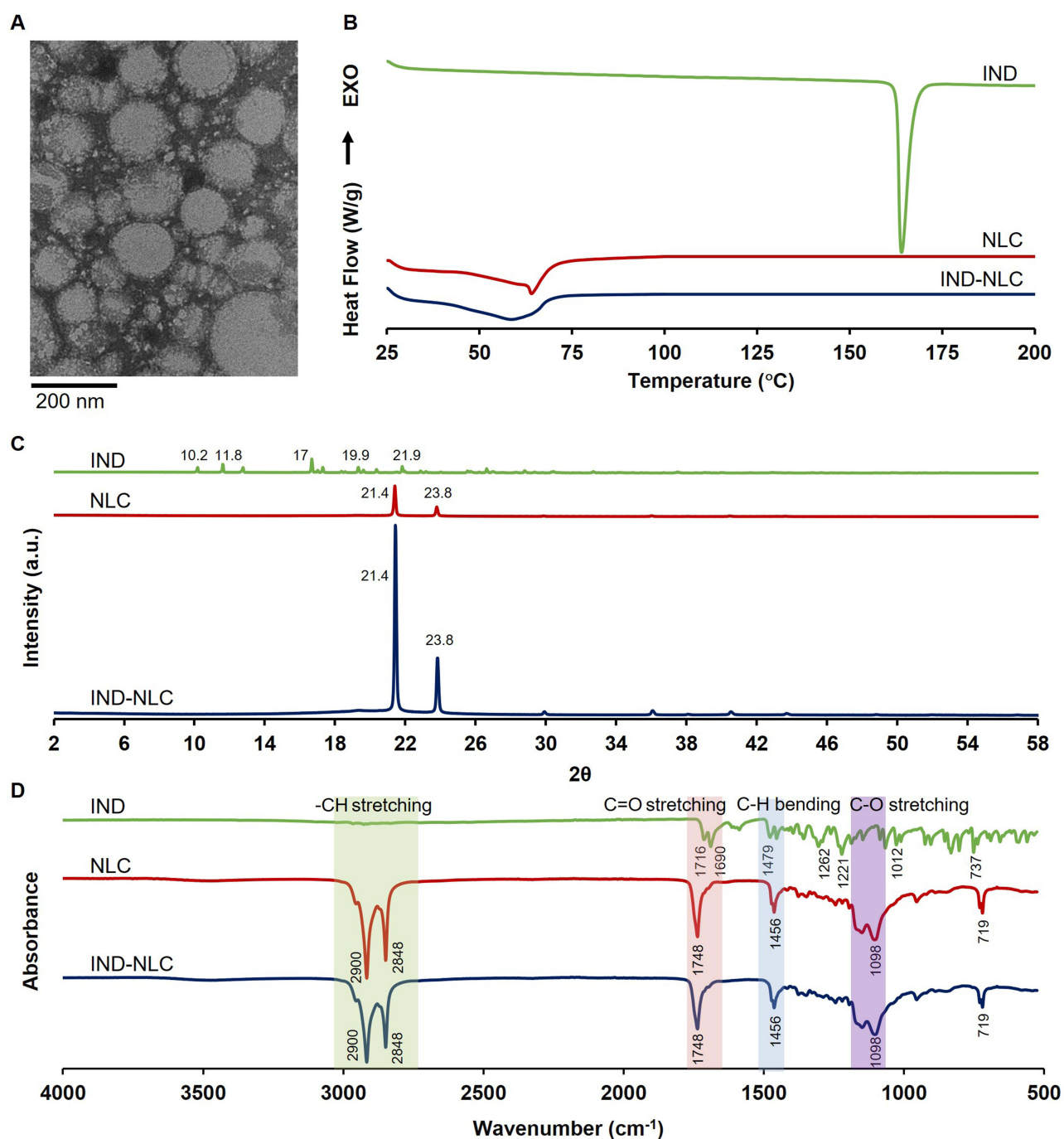


**Figure 1** Morphological and physicochemical characterization of IND-NLC: **(A)** TEM image of IND-NLC, **(B)** DSC, **(C)** XRD and **(D)** ATR-FTIR studies of IND, empty NLC and IND-NLC.

from  $166 \pm 1.9$  nm to  $165.1 \pm 1.4$  nm, PDI was below 0.2 and ZP values decreased from  $-30 \pm 0.3$  to  $-28.2 \pm 0.3$  mV. Additionally, the EE was maintained at  $99.44 \pm 0.02\%$ . These results indicate that gamma irradiation had no significant effects on the physicochemical parameters of IND-NLC.

## Biopharmaceutical Behaviour of Nanoformulation Loading Indomethacin

The *in vitro* release of IND from IND-NLC was measured for 24 h at 37 °C and compared against free IND. Free IND reached equilibrium (100% release) after 10 hours, whereas IND-NLC displayed slower release of drug only on the level



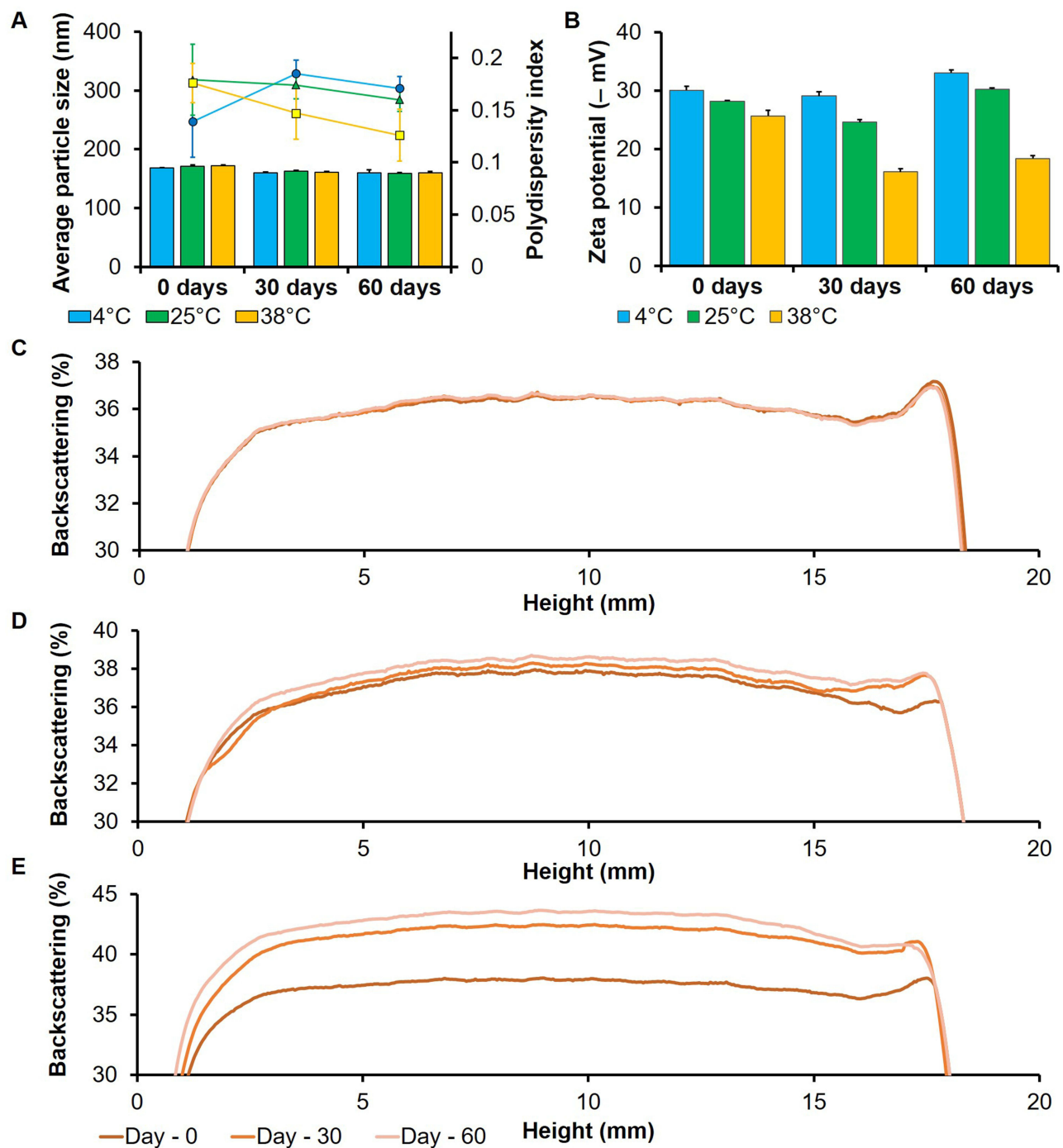


**Figure 2** Storage stability of IND-NLC at different temperatures (4, 25 and 37 °C): **(A)** Average particle size (bars) and Polydispersity index (lines), **(B)** Zeta potential and **(C-E)** Backscattering profiles of IND-NLC measured during 60 days at 4, 25 and 38 °C, respectively. Data are presented as mean  $\pm$  standard deviation ( $n=3$ ).

of 25% after 10 hours, which increased up to 31% after 24 hours. In addition, the release curves were fitted to several kinetic models (Table 1), and the best fit was assigned for IND and IND-NLC by first-order ( $r^2=0.97$ ;  $k_f=0.41$ ) and hyperbolic models ( $r^2=0.99$ ,  $k_m=5.24$ ,  $V_m = 40.2$ ), respectively (Figure 4).

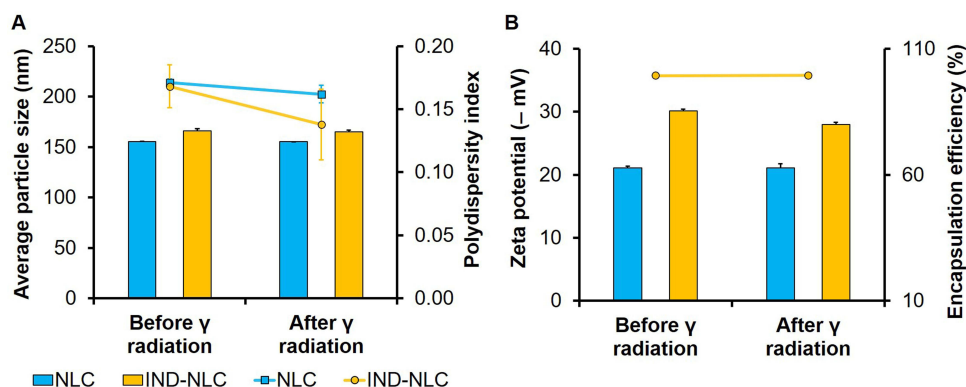


**Figure 3** Effect of gamma radiation on physicochemical properties of IND-NLC: (A) Average particle size (bars), and Polydispersity index (lines), (B) Zeta potential (bars) and Encapsulation efficiency (lines) values of empty NLC and IND-NLC before and after gamma radiation. Data are presented as mean  $\pm$  standard deviation ( $n=3$ ).

## Antiproliferative Activity Towards Selected Cancer Cell Lines

The results of the inhibitory action of IND-NLC on the growth of breast (MDA-MB-468) and prostate (PC-3) cancer cells are presented in Table 2. The results are expressed as the IC<sub>50</sub> concentration of the drug in IND-NLC, or as free drug (in  $\mu\text{M}$ ), that reduces cell proliferation by 50% compared to the untreated cells (control).

The antiproliferative activity of indomethacin delivered via the IND-NLC nanotechnological system was significantly higher than that of free IND. During the first 24 hours of incubation, IND-NLC did not exhibit activity. This activity emerged after 48 hours, when IND-NLC demonstrated the ability to inhibit prostate and breast cancer cells at concentrations 74.1  $\mu\text{M}$  and 15.7  $\mu\text{M}$ , respectively, at which free IND showed no activity.

**Table 1** In vitro IND and IND-NLC Release Data Fitted to the Most Common Kinetic Models

Kinetic Models	Values	Free IND	IND-NLC
Zero-order	R <sup>2</sup>	0.13	0.23
	K <sub>0</sub>	7.27	1.98
First-order	R <sup>2</sup>	0.97	0.97
	K <sub>f</sub>	0.41	0.19
Hyperbola	R <sup>2</sup>	0.90	0.99
	K <sub>m</sub>	3.42	5.24
	V <sub>m</sub>	134.1	40.2
Higuchi	R <sup>2</sup>	0.70	0.90
	K <sub>h</sub>	28.23	7.83
Korsmeyer-Peppas	R <sup>2</sup>	0.74	0.90
	K <sub>kp</sub>	36.09	8.29
	n	0.41	0.47

**Notes:** K<sub>0</sub>, K<sub>f</sub>, K<sub>m</sub>, K<sub>h</sub>, K<sub>0</sub>, V<sub>m</sub> and n represent zero-order, first-order, hyperbolic, Higuchi, Korsmeyer-Peppas release rate constants, maximum release speed, and release exponent, respectively.

**Abbreviations:** IND, indomethacin; IND-NLC, indomethacin-loaded nanostructured lipid carriers.

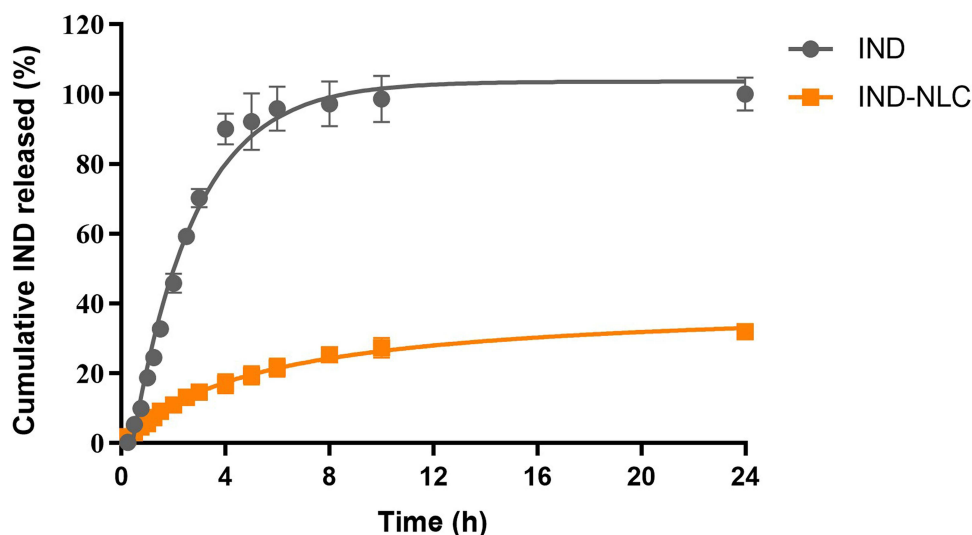


**Figure 4** In vitro release profile of free IND and IND-NLC. Data adjusted to the best fitted models being first-order and hyperbola models, respectively. Data are displayed as mean  $\pm$  standard deviation (n=3).

## Accumulation of Nanocarriers Loading Indomethacin in Cancer Cells

Flow cytometry was used to determine the ability of IND-NLC to accumulate in the MDA-MB-468 and PC-3 cancer cell lines. The fluorescent dye Nile red (NR) was used to visualise this process as a pigment that binds neutral fat and phospholipids. Cells of both lines were incubated with fluorescently labeled IND-NLC and analyzed at several time points. The results are presented in Figure 5. Cell fluorescence was analyzed by comparing the shifts of histograms reported for labeled and unlabeled cells. The accumulation of nanoparticles in PC-3 cells was rapid between 5 minutes and 1 hour, and then remained stable without any changes in fluorescence intensity between 2 and 4 hours. In breast cancer cells, the accumulation of NLC increased over time, as shown in Figure 5 by the increasing fluorescence intensity from 5 minutes to 4 hours.

## Discussion

Indomethacin (IND) is a widely used oral nonsteroidal anti-inflammatory drug (NSAID) that acts via nonspecific inhibition of COX enzymes (COX-1 and COX-2). Its anticancer potential was for the first time observed by Stoll, who reported that the daily administration of IND (100 and 150 mg) almost completely reduced a group of metastatic chest wall nodules in breast

**Table 2** Half Maximal Inhibitory Concentrations ( $IC_{50}$ ) of NLC and IND-NLC Against Selected Cancer Cell Lines

Compound and Formulations	Cell lines $IC_{50}$ [ $\mu M$ ]			
	PC-3		MDA-MB-468	
	24 h	48 h	24 h	48 h
NLC	NA	14.9 $\pm$ 5.6	NA	69.6 $\pm$ 27.5
IND-NLC	NA	74.1 $\pm$ 30.9	NA	15.7 $\pm$ 2.2

**Notes:** Data are presented as the mean  $\pm$  standard deviation (SD) calculated using the Prolab-3 system based on Cheburator 0.4 software. The statistical analysis for two-group comparisons, NLC vs IND-NLC, was performed by using non-parametric Mann-Whitney test, GraphPad Prism 7. A statistically significant difference was considered at  $p \leq 0.05$ . NA- non active in the range of 0.8–100  $\mu M$ .

**Abbreviations:** NLC, nanostructured lipid carriers; IND-NLC, indomethacin-loaded nanostructured lipid carriers; PC-3, prostate cancer cell line; MDA-MB-468, triple-negative human breast cancer cell line.

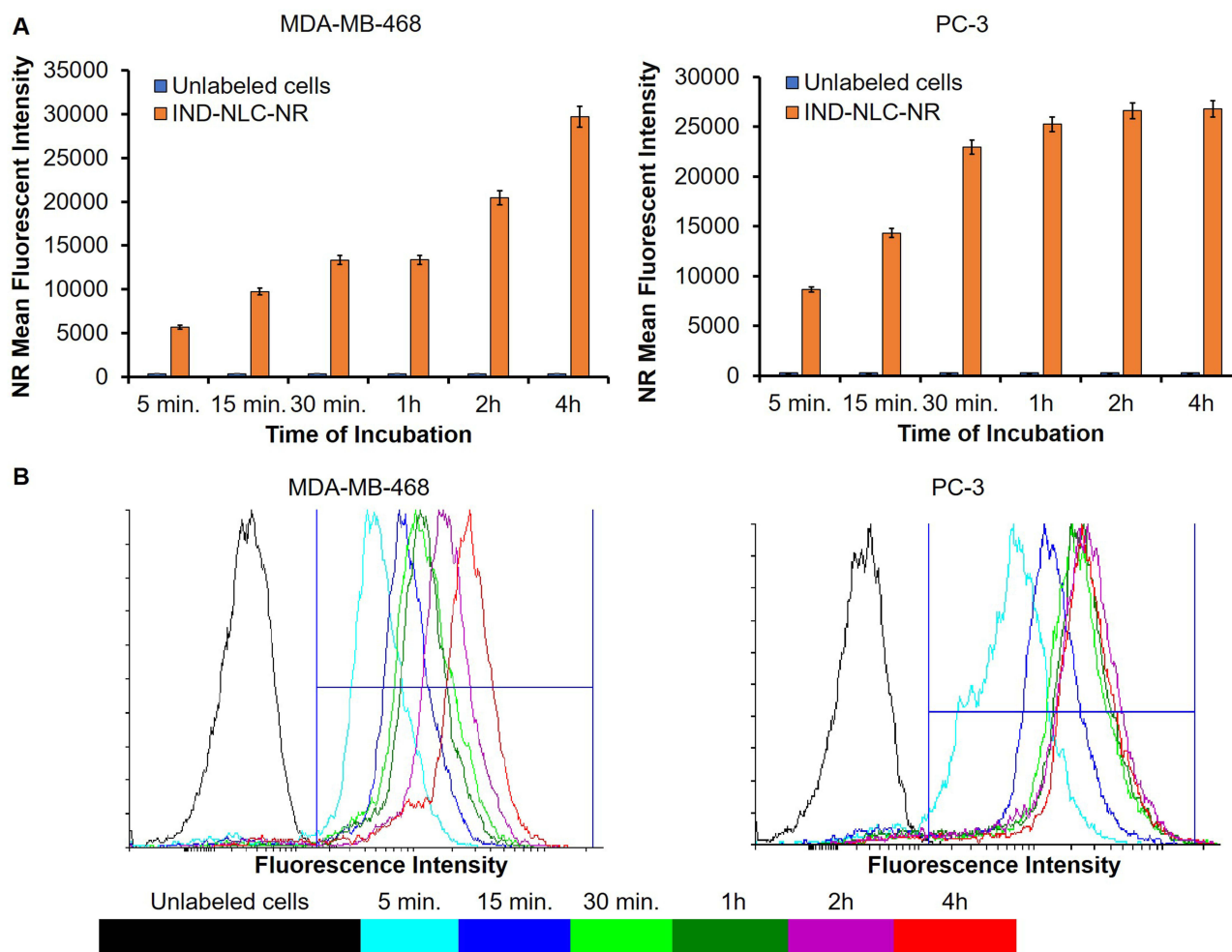


**Figure 5** Accumulation of IND-NLC in PC-3 and MDA-MB-468 cells. **(A)** Mean fluorescent intensity after 5, 15, 30 minutes and 1, 2 and 4 hours; **(B)** Flow cytometry histograms of IND-NLC-NR.

cancer.<sup>36</sup> Despite many positive results in in vitro and in vivo tests, the use of IND as a chemopreventive and cytostatic agent has not been feasible due to several undesirable side effects. Oral delivery of IND is also limited by several factors, such as its poor water solubility (105.2  $\mu\text{g}/\text{mL}$  at  $\text{pH} = 7$ ), low absorption, and COX-1 independent gastrointestinal side-effects.<sup>37,38</sup> Therefore, the aim of this study was to create a novel delivery system that incorporates IND and improves its effectiveness against cancer. IND-NLC were effectively produced using the hot high-pressure homogenization technique, which is commonly employed in the pharmaceutical industry. Beeswax and Miglyol<sup>®</sup> 812 were used for the production of nanoparticles as solid and liquid lipids, respectively, and as a result, we obtained IND-NLC with negative charge ( $-30.1$  mV), size of 168.1 nm, and PDI of 0.139. IND-NLC showed high EE over 99%, attributed to the lipophilic properties of IND, showing affinity to the lipid-based internal structure of the NLC.

NLC should be able to bypass blood clearance and mononuclear phagocyte system (MPS). From these aspects, the physicochemical and morphological parameters of NLCs are of utmost importance. Particles smaller than 5 nm are effectively removed by the kidneys and eliminated through urine, but bigger particles, ranging from 20 to 100 nm, are either taken up by macrophages or stored in healthy tissues, which hinders their ability to reach the intended target.<sup>39,40</sup> In this area, several strategies had been employed such as hydrogels combination with photothermal therapy or even surface-coating with specific molecules.<sup>41,42</sup> Based on this, we fabricated the particles with size ranged within 150–200 nm. Furthermore, we focused on the surface charges of nanoparticles. Cationic particles are identified by MPS faster than anionic or neutral ones.<sup>40</sup> Anionic particles could prevent toxic effects in blood circulation that are connected to cationic charge mediated adsorption of blood proteins on the surface.<sup>43</sup> Negatively charged particles may also reduce the non-specific uptake by liver.<sup>44</sup> Nanocarriers of this

kind exhibit excellent cellular internalisation and, owing to their extended blood circulation duration, they are more efficiently dispersed within tumors compared to nanocarriers of the same size but with a positive surface charge.<sup>45</sup> However, it has been reported in the literature that they exhibit a rapid accumulation in the lung.<sup>45</sup> A good deal of data suggest that highly charged nanoparticles have a significantly higher opsonisation rates compared to neutral or slightly surface-charged nanoparticles of the same size. The relatively low uptake of slightly negatively charged nanoparticles from the liver can be explained by the low rate of opsonisation and the electrostatic repulsion, which reduce macrophages recognition and non-specific uptake.<sup>46</sup>

In addition to DLS results, visual TEM observation confirmed spherical and lipid nanoparticles with average size below 200 nm (Figure 1A). The uniform particle size in the TEM images confirmed that the PDI values obtained were similar to the visual observations. Moreover, spherical nanoparticles are reported to undergo cellular endocytosis faster than any other shapes.<sup>40</sup>

The interaction between the drug and lipid matrix was studied by DSC (Figure 1B), and it was confirmed that IND was successfully incorporated into the NLC. Similar melting points between NLC and IND-NLC indicate that the drug is well homogenized in the lipid matrix.<sup>47</sup>

XRD analysis provided information regarding the molecular dispersion of IND inside NLC (Figure 1C). Two new peaks that appeared in the spectrum of IND-NLC at 21.4° and 23.8° (2θ) were also observed in the empty NLC, confirming the orthorhombic subcell diffraction of the waxes.<sup>33</sup>

Fourier-transform infrared spectroscopy (FTIR) proved the lack of covalent bonds between indomethacin and the lipid matrix (Figure 1D). The main peaks characteristic of empty NLC were also observed for IND-NLC formulation. In the fingerprint region of beeswax, 719–1098 cm<sup>-1</sup> in both spectra are visible bond vibrations corresponding to CH<sub>2</sub> rocking, C-H bending, and C=O stretching of hydrocarbons, esters, and free fatty acids in beeswax. The major vibrations occurring between 2848 and 2900 cm<sup>-1</sup> are the result of the symmetrical and asymmetrical stretching vibrations of the CH<sub>2</sub> groups of the hydrocarbon molecules found in the solid lipid.

The release of drugs from IND-NLC is a crucial parameter and directly determines therapeutic efficacy. The release profile of IND was determined after 24 hours. Results presented in Figure 4 demonstrate a faster release of free IND compared with IND-NLC. After 10 hours, free IND was fully released, whereas at the same time, IND release from NLC reached only 25%. During the first time point, a burst release of IND from NLC was observed, but later, a prolonged release of IND was produced. These observations may be the consequence of an initial release of IND attached to the NLC outer lipid core, followed by a slower release of inner encapsulated IND. This is confirmed by the data presented in Table 1, which best fits a hyperbola model.<sup>48</sup> Presented release is related to prolonged release and may be suitable as a parenteral drug delivery system.<sup>47</sup>

HPH stabilises the interfacial tension and produces a stable hydrodynamic NLC size over the long term.<sup>49</sup> However, the storage stability of nanoparticles ensures the quality of the formulation.<sup>50</sup> In this sense, we demonstrated stable physicochemical parameters of IND-NLC over 60 days (Figure 2A and B) at refrigeration (4 °C) and room temperature (25 °C). The stability of IND-NLC was evaluated by measuring Z-Ave, PDI, and ZP as well as by analyzing the backscattering (BS) profile. For this last purpose, we used Turbiscan<sup>®</sup> analysis, which is considered a useful technique to identify physical changes in advance such as sedimentation, creaming, size variation, flocculation, and coalescence.<sup>51</sup> BS provides the information about destabilization mechanism such as sedimentation, agglomeration, or aggregation that can be observed when the difference is greater than 10%.<sup>52</sup> Results obtained in Figure 2C–E demonstrate that the most suitable method to store IND-NLC is at 4 °C, where the formulation was stable for 60 days since the physicochemical parameters were maintained. These observations are in accordance with the results obtained from Turbiscan<sup>®</sup> as well as with literature data, which indicates that nanoparticles are more stable at 4 °C than at 25 °C.<sup>53</sup>

The potential of IND as a cancer treatment has been described in several reports, all of which indicate a lack of viability for wider use in anticancer therapy due to the presence of side effects during clinical experiments.<sup>54,55</sup> Using nanotechnological techniques, we developed IND-NLC and evaluated their antiproliferative activity against two selected cancer cell lines. Studies were carried out against prostate (PC-3) and breast (MDA-MB-468) cancer cell lines. These types of cancer were selected based on the scale of the health problems they generated. Prostate cancer (PC) is the second most common cancer among men worldwide<sup>56</sup> and one of the leading causes of cancer-related death.<sup>57</sup> Triple-negative breast cancer (TNBC) has the worst survival prognosis among breast cancer cases.<sup>58</sup> The absence of a response to normal hormonal therapy or drugs targeting specific receptors (eg, HER2) makes the management of this condition difficult.<sup>59</sup>



IND-NLC formulation showed high cytotoxicity against both studied cancer cell lines PC-3 and MB-468 (Table 2). During the first 24 h, empty and IND-NLC did not exert antitumoral effects. Antitumor activity was noted after 48 hours where IND-NLC effectively inhibited prostate and breast cancer cell proliferation at concentrations of 74.1  $\mu\text{M}$  and 15.7  $\mu\text{M}$ , respectively. At the same timepoints and concentrations, free IND failed to show cytotoxicity. Differences regarding IND-NLC activity in both cell lines may be attributed to their different sensitivity to IND-NLC. In the case of breast cancer cells, we observed that they proliferate significantly faster compared to PC-3 cells, which may contribute to their increased sensitivity. This improved cytotoxic capacity may be due to an enhanced absorption of IND-NLC, as demonstrated in the subsequent phase of the study. Additionally, it could also result from the synergic effects between IND and the lipid components in the formulation. Miglyol<sup>®</sup> 812 is a pharmacological product of the glycerol triester of caprylic acid and capric acid, which have been claimed to exert cytotoxic and cancer gene regulatory effects,<sup>60</sup> whereas beeswax is reported to possess cytotoxic, apoptotic, anti-angiogenic, and anti-metastatic properties towards human tumor cell lines.<sup>21,22</sup>

Cellular uptake studies of IND-NLC were evaluated using the fluorescent dye NR and proved that nanoparticles with encapsulated drug are able to penetrate cancer cells. Flow cytometry confirmed rapid cellular uptake of IND-NLC-NR especially in the case of PC-3 cells (Figure 5B). Moreover, the fluorescence intensity increased during the study, and the highest signals were observed after 4 hours and 2 hours for breast and prostate cancer cells, respectively. These results confirm that lipid nanoparticles effectively penetrate cell lipid membranes probably due to their lipid structure,<sup>61,62</sup> the presence of liquid lipids in the formulation, their spherical shape, and reduced size.<sup>63</sup>

## Conclusion

In summary, we successfully developed nanostructured lipid carriers (NLC) loaded with indomethacin (IND), achieving suitable physicochemical parameters. IND-NLC demonstrated high stability, high encapsulation efficacy, and controlled release of indomethacin. Additionally, encapsulation of IND in NLC significantly enhanced its anticancer activity, possibly through a synergistic interaction with the cytotoxic activity of beeswax, which was deliberately used as a solid lipid component in the formulation. Consequently, even the empty NLC showed cytotoxic effects. Based on these findings, NLC loaded with indomethacin constitutes a promising system for supporting cancer treatment. However, further detailed preclinical and clinical studies are essential to validate the efficacy of this therapy. For future directions, it will be crucial to investigate the mechanism of action of these nanoparticles at the cellular and molecular levels, as well as to explore their biodistribution and pharmacokinetics in vivo.

## Acknowledgments

This work was supported by the Wrocław University of Environmental and Life Sciences (Poland) under the Ph.D. research programme “Innovative Doctorate” no. N070/0005/22.

The article is part of a PhD dissertation titled “Development of lipid nanosystems of nonsteroidal anti-inflammatory drugs (NSAIDs) and their multifunctional bioconjugates for targeting cancer treatment”, prepared during Doctoral School at the Wrocław University of Environmental and Life Sciences. The APC/BPC is financed/co-financed by Wrocław University of Environmental and Life Sciences.

## Disclosure

The authors report no conflicts of interest in this work.

## References

1. Global cancer burden growing, amidst mounting need for services. Available from: <https://www.who.int/news/item/01-02-2024-global-cancer-burden-growing-amidst-mounting-need-for-services>. Accessed March 24, 2024.
2. Prasad V, Mailankody S. Research and development spending to bring a single cancer drug to market and revenues after approval. *JAMA Intern Med.* 2017;177(11):1569. doi:10.1001/JAMAINTERNMED.2017.3601
3. Novel drug approvals for 2023 | FDA. Available from: <https://www.fda.gov/drugs/new-drugs-fda-cders-new-molecular-entities-and-new-therapeutic-biological-products/novel-drug-approvals-2023>. Accessed January 4, 2024.
4. EMA. Available from: <https://www.ema.europa.eu/en/news/human-medicines-highlights-2022>. Accessed May 27, 2023.
5. Zhou JX, Torres VE. Drug repurposing in autosomal dominant polycystic kidney disease. *Kidney Int.* 2023;103(5):859–871. doi:10.1016/J.KINT.2023.02.010

6. Wong RSY. Role of Nonsteroidal Anti-Inflammatory Drugs (NSAIDs) in cancer prevention and cancer promotion. *Adv Pharmacol Sci.* 2019;4:2.
7. Pollard M, Luckert PH, Schmidt MA. The suppressive effect of piroxicam on autochthonous intestinal tumors in the rat. *Cancer Lett.* 1983;21(1):57–61.
8. Coogan PF, Rosenberg L, Palmer JR, et al. Nonsteroidal anti-inflammatory drugs and risk of digestive cancers at sites other than the large bowel. *Cancer Epidemiol Biomarkers Prev.* 2000;9(1):119–123.
9. Suri A, Sheng X, Schuler KM, et al. The effect of celecoxib on tumor growth in ovarian cancer cells and a genetically engineered mouse model of serous ovarian cancer. *Oncotarget.* 2016;7(26):39582. doi:10.18632/ONCOTARGET.8659
10. Ravichandran R, Mohan SK, Sukumaran SK, et al. An open label randomized clinical trial of Indomethacin for mild and moderate hospitalised Covid-19 patients. *Sci Rep.* 2022;12(1):1–10. doi:10.1038/s41598-022-10370-1
11. Eli Y, Przeddecki F, Levin G, Kariv N, Raz A. Comparative effects of indomethacin on cell proliferation and cell cycle progression in tumor cells grown in vitro and in vivo. *Biochem Pharmacol.* 2001;61(5):565–571. doi:10.1016/S0006-2952(00)00578-5
12. Palazzolo S, Bayda S, Hadla M, et al. The clinical translation of organic nanomaterials for cancer therapy: a focus on polymeric nanoparticles, micelles, liposomes and exosomes. *Curr Med Chem.* 2018;25(34):4224–4268. doi:10.2174/0929867324666170830113755
13. O'Brien MER, Wigler N, Inbar M, et al. Reduced cardiotoxicity and comparable efficacy in a phase III trial of pegylated liposomal doxorubicin HCl (CAELYX™/Doxil®) versus conventional doxorubicin for first-line treatment of metastatic breast cancer. *Ann Oncol.* 2004;15(3):440–449. doi:10.1093/ANNONC/MDH097
14. Kalyane D, Raval N, Maheshwari R, Tambe V, Kalia K, Tekade RK. Employment of enhanced permeability and retention effect (EPR): nanoparticle-based precision tools for targeting of therapeutic and diagnostic agent in cancer. *Mater Sci Eng C.* 2019;98:1252–1276. doi:10.1016/J.MSEC.2019.01.066
15. Sarvepalli S, Parvathani V, Chauhan G, Shukla SK, Gupta V. Inhaled indomethacin-loaded liposomes as potential therapeutics against Non-Small Cell Lung Cancer (NSCLC). *Pharm Res.* 2022;39(11):2801–2815. doi:10.1007/S11095-022-03392-X/FIGURES/8
16. Hippalgaonkar K, Adelli GR, Hippalgaonkar K, Repka MA, Majumdar S. Indomethacin-loaded solid lipid nanoparticles for ocular delivery: development, characterization, and in vitro evaluation. *J Ocul Pharmacol Ther.* 2013;29(2):216–228. doi:10.1089/JOP.2012.0069
17. Balguri SP, Adelli GR, Majumdar S. Topical ophthalmic lipid nanoparticle formulations (SLN, NLC) of indomethacin for delivery to the posterior segment ocular tissues. *Eur J Pharm Biopharm.* 2016;109:224–235. doi:10.1016/J.EJPB.2016.10.015
18. Salvi VR, Pawar P. Nanostructured lipid carriers (NLC) system: a novel drug targeting carrier. *J Drug Deliv Sci Technol.* 2019;51:255–267. doi:10.1016/J.JDDST.2019.02.017
19. Chauhan I, Yasir M, Verma M, Singh AP. Nanostructured lipid carriers: a groundbreaking approach for transdermal drug delivery. *Adv Pharm Bull.* 2020;10(2):150–165. doi:10.34172/APB.2020.021
20. Leonida MD, Kumar I. Bionanomaterials for skin regeneration. *Switz Springer Int Publ;* 2016. Available from: <http://link.springer.com>. Accessed July 5, 2024.
21. Choudhari MK, Haghniaz R, Rajwade JM, Paknikar KM. Anticancer activity of Indian stingless bee propolis: an in vitro study. *Evid Based Complement Altern Med.* 2013;2013:10. doi:10.1155/2013/928280
22. Forma E, Bryś M. Anticancer Activity of Propolis and Its Compounds. *Nutrients.* 2021;13(8):2594. doi:10.3390/NU13082594
23. Thiruchenthooran V, Świtalska M, Bonilla L, et al. Novel strategies against cancer: dexibuprofen-loaded nanostructured lipid carriers. *Int J Mol Sci.* 2022;23(19):2.
24. Lacerda SP, Cerize NNP, Ré MI. Preparation and characterization of carnauba wax nanostructured lipid carriers containing benzophenone-3. *Int J Cosmet Sci.* 2011;33(4):312–321. doi:10.1111/J.1468-2494.2010.00626.X
25. Sánchez-López E, Etcheto M, Egea MA, et al. New potential strategies for Alzheimer's disease prevention: pegylated biodegradable dexibuprofen nanospheres administration to APP<sup>swE/PS1dE9</sup>. *Nanomed Nanotechnol Biol Med.* 2017;13(3):1171–1182. doi:10.1016/J.NANO.2016.12.003
26. Li Y, Chen Y, Liu R, et al. Study on contrast-enhanced ultrasound imaging and anti-tumor effects of drug-loaded nanodroplets with tumor targeting and ultrasound sensitivity. *Front Biosci.* 2023;28(6):115. doi:10.31083/J.FBL2806115/0F40F41AC5BB7DB39E9931B39CD310D0.PDF
27. Abila MJ, Banga AK. Formulation of tocopherol nanocarriers and in vitro delivery into human skin. *Int J Cosmet Sci.* 2014;36(3):239–246. doi:10.1111/ICS.12119
28. El-Houssieny BM, ei E-DEZ, El-Messiry HM. Enhancement of solubility of dexibuprofen applying mixed hydrotropic solubilization technique. *Drug Discov Ther.* 2014;8(4):178–184.
29. Carvajal-Vidal P, González-Pizarro R, Araya C, et al. Nanostructured lipid carriers loaded with Halobetasol propionate for topical treatment of inflammation: development, characterization, biopharmaceutical behavior and therapeutic efficacy of gel dosage forms. *Int J Pharm.* 2020;585:119480. doi:10.1016/J.IJPHARM.2020.119480
30. Gliszczynska A, Świtalska M, Wietrzyk J, Wawrzęńczyk C. Synthesis of a natural  $\gamma$ -butyrolactone from nerylacetone by Acremonium roseum and Fusarium oxysporum cultures. *Nat Prod Commun.* 2011;6(3):367–370. doi:10.1177/1934578x1100600313
31. Nevozhay D. Cheburator software for automatically calculating drug inhibitory concentrations from in vitro screening assays. *PLoS One.* 2014;9(9):e106186. doi:10.1371/JOURNAL.PONE.0106186
32. Surwase SA, Boetker JP, Saville D, et al. Indomethacin: new polymorphs of an old drug. *Mol Pharm.* 2013;10(12):4472–4480. doi:10.1021/MP400299A/SUPPL\_FILE/MP400299A\_SI\_001.PDF
33. Jenning V, Gohla S. Comparison of wax and glyceride solid lipid nanoparticles (SLN®). *Int J Pharm.* 2000;196(2):219–222. doi:10.1016/S0378-5173(99)00426-3
34. Jamrógiewicz M, Józefowicz M. Preparation and characterization of indomethacin supramolecular systems with  $\beta$ -Cyclodextrin in order to estimate photostability improvement. *Molecules.* 2021;26(24):7436. doi:10.3390/MOLECULES26247436
35. Gainza G, Pastor M, Aguirre JJ, et al. A novel strategy for the treatment of chronic wounds based on the topical administration of rhEGF-loaded lipid nanoparticles: in vitro bioactivity and in vivo effectiveness in healing-impaired db/db mice. *J Control Release.* 2014;185(1):51–61. doi:10.1016/J.JCONREL.2014.04.032
36. Stoll BA. Indomethacin in breast cancer. *Lancet.* 1973;2(7825):384. doi:10.1016/S0140-6736(73)93234-0
37. Tres F, Treacher K, Booth J, et al. Indomethacin-kollidon VA64 extrudates: a mechanistic study of pH-dependent controlled release. *Mol Pharm.* 2016;13(3):1166–1175. doi:10.1021/ACS.MOLPHARMACEUT.5B00979/SUPPL\_FILE/MP5B00979\_SI\_001.PDF
38. Althobaiti AA, Ashour EA, Almutairi A, Almutairi M, AlYahya M, Repka MA. Development and characterization of different dosage forms of nifedipine/indomethacin fixed-dose combinations. *J Drug Deliv Sci Technol.* 2023;80. doi:10.1016/J.JDDST.2022.104117

39. Jasinski DL, Li H, Guo P. The effect of size and shape of RNA nanoparticles on biodistribution. *Mol Ther*. 2018;26(3):784–792. doi:10.1016/J.YMTHE.2017.12.018
40. Di J, Gao X, Du Y, Zhang H, Gao J, Zheng A. Size, shape, charge and “stealthy” surface: carrier properties affect the drug circulation time in vivo. *Asian J Pharm Sci*. 2021;16(4):444–458. doi:10.1016/J.AJPS.2020.07.005
41. Li B, Wang W, Zhao L, et al. Photothermal therapy of tuberculosis using targeting pre-activated macrophage membrane-coated nanoparticles. *Nat Nanotechnol*. 2024;2024:1–12. doi:10.1038/s41565-024-01618-0
42. Shen W, Pei P, Zhang C, et al. A polymeric hydrogel to eliminate programmed death-ligand 1 for enhanced tumor radio-immunotherapy. *ACS Nano*. 2023;17(23):23998–24011. doi:10.1021/ACS.NANO.3C08875/SUPPL\_FILE/NN3C08875\_SI\_001.PDF
43. Doshi N, Mitragotri S. Macrophages recognize size and shape of their targets. *PLoS One*. 2010;5(4):e10051. doi:10.1371/JOURNAL.PONE.0010051
44. Xiao K, Li Y, Luo J, et al. The effect of surface charge on in vivo biodistribution of PEG-oligocholeic acid based micellar nanoparticles. *Biomaterials*. 2011;32(13):3435–3446. doi:10.1016/J.BIOMATERIALS.2011.01.021
45. He C, Hu Y, Yin L, Tang C, Yin C. Effects of particle size and surface charge on cellular uptake and biodistribution of polymeric nanoparticles. *Biomaterials*. 2010;31(13):3657–3666. doi:10.1016/J.BIOMATERIALS.2010.01.065
46. Dobrovolskaia MA, Aggarwal P, Hall JB, McNeil SE. Preclinical studies to understand nanoparticle interaction with the immune system and its potential effects on nanoparticle biodistribution. *Mol Pharm*. 2008;5(4):487–495. doi:10.1021/MP800032F/ASSET/IMAGES/MEDIUM/MP-2008-00032F\_0005.GIF
47. Muller RH, Ranjita S, Cornelia MK. 20 Years of Lipid Nanoparticles (SLN & NLC): present state of development & industrial applications. *Curr Drug Discov Technol*. 2011;8(3):207–227.
48. Yang X, Han M, Wang X, et al. Evaluation of the synergistic effects of epigallocatechin-3-gallate-loaded PEGylated-PLGA nanoparticles with nimodipine against neuronal injury after subarachnoid hemorrhage. *Front Nutr*. 2023;9:953326. doi:10.3389/FNUT.2022.953326/BIBTEX
49. Gramdorf S, Hermann S, Hentschel A, et al. Crystallized miniemulsions: influence of operating parameters during high-pressure homogenization on size and shape of particles. *Colloids Surf a Physicochem Eng Aspects*. 2008;331(1–2):108–113. doi:10.1016/J.COLSURFA.2008.07.016
50. Kovács A, Berkó S, Csányi E, Csóka I. Development of nanostructured lipid carriers containing salicylic acid for dermal use based on the Quality by Design method. *Eur J Pharm Sci*. 2017;99:246–257. doi:10.1016/J.EJPS.2016.12.020
51. Celia C, Trapasso E, Cosco D, Paolino D, Fresta M. Turbiscan Lab<sup>®</sup> Expert analysis of the stability of ethosomes<sup>®</sup> and ultradeformable liposomes containing a bilayer fluidizing agent. *Colloids Surf B Biointerfaces*. 2009;72(1):155–160. doi:10.1016/J.COLSURFB.2009.03.007
52. Stability of Dispersions | 3P Instruments. Available from: <https://www.3p-instruments.com/measurement-methods/stability-turbiscan/>. Accessed December 13, 2023.
53. Bonilla-Vidal L, Świtalska M, Espina M, et al. Dually active apigenin-loaded nanostructured lipid carriers for cancer treatment. *Int J Nanomed*. 2023;18:6979–6997. doi:10.2147/IJN.S429565
54. Gentile LB, Queiroz-Hazarbassanov N, Massoco CDO, Fecchio D. Modulation of cytokines production by indomethacin acute dose during the evolution of Ehrlich Ascites tumor in mice. *Mediators Inflamm*. 2015;2015. doi:10.1155/2015/924028
55. Gliszczyńska A, Nowaczyk M. Lipid formulations and bioconjugation strategies for indomethacin therapeutic advances. *Molecules*. 2021;26(6):1576. doi:10.3390/MOLECULES26061576
56. Siegel RL, Miller KD, Jemal A. Cancer Statistics, 2020. *CA Cancer J Clin*. 2020;70(1):7–30. doi:10.3322/caac.21590
57. Sung H, Ferlay J, Siegel RL, et al. Global Cancer statistics 2020: GLOBOCAN estimates of incidence and mortality worldwide for 36 cancers in 185 countries. *CA Cancer J Clin*. 2021;71(3):209–249. doi:10.3322/CAAC.21660
58. DeSantis CE, Fedewa SA, Goding Sauer A, Kramer JL, Smith RA, Jemal A. Breast cancer statistics, 2015: convergence of incidence rates between black and white women. *CA Cancer J Clin*. 2016;66(1):31–42. doi:10.3322/caac.21320
59. Skandan SP. 5 year Overall survival of triple negative breast cancer: a single institution experience. *J Clin Oncol*. 2016;34(15\_suppl). doi:10.1200/JCO.2016.34.15\_SUPPL.E12580
60. Narayanan A, Baskaran SA, Amalaradjou MAR, Venkitanarayanan K. Anticarcinogenic properties of medium chain fatty acids on human colorectal, skin and breast cancer cells in vitro. *Int J Mol Sci*. 2015;16(3):5014–5027. doi:10.3390/ijms16035014
61. Strachan JB, Dyett BP, Nasa Z, Valery C, Conn CE. Toxicity and cellular uptake of lipid nanoparticles of different structure and composition. *J Colloid Interface Sci*. 2020;576:241–251. doi:10.1016/J.JCIS.2020.05.002
62. Zhang W, Liu J, Zhang Q, et al. Enhanced cellular uptake and anti-proliferating effect of chitosan hydrochlorides modified genistein loaded NLC on human lens epithelial cells. *Int J Pharm*. 2014;471(1–2):118–126. doi:10.1016/J.IJPHARM.2014.05.030
63. Neves AR, Queiroz JF, Costa Lima SA, Figueiredo F, Fernandes R, Reis S. Cellular uptake and transcytosis of lipid-based nanoparticles across the intestinal barrier: relevance for oral drug delivery. *J Colloid Interface Sci*. 2016;463:258–265. doi:10.1016/j.jcis.2015.10.057

International Journal of Nanomedicine

Dovepress

Publish your work in this journal

The International Journal of Nanomedicine is an international, peer-reviewed journal focusing on the application of nanotechnology in diagnostics, therapeutics, and drug delivery systems throughout the biomedical field. This journal is indexed on PubMed Central, MedLine, CAS, SciSearch<sup>®</sup>, Current Contents<sup>®</sup>/Clinical Medicine, Journal Citation Reports/Science Edition, EMBASE, Scopus and the Elsevier Bibliographic databases. The manuscript management system is completely online and includes a very quick and fair peer-review system, which is all easy to use. Visit <http://www.dovepress.com/testimonials.php> to read real quotes from published authors.

Submit your manuscript here: <https://www.dovepress.com/international-journal-of-nanomedicine-journal>